Journal of *Marine Science and Engineering*

MDPI

Article

Assessing the Effectiveness of Regional Storm Surge Reduction Strategies and Tank Level Structural Mitigation Measures for Aboveground Storage Tanks

Santosh Ghimire and Sabarethinam Kameshwar *

Department of Civil and Environmental Engineering, College of Engineering, Louisiana State University, Baton Rouge, LA 70803, USA; sghim11@lsu.edu

* Correspondence: skameshwar1@lsu.edu

Abstract: The effectiveness of regional storm surge reduction strategies and tank-level structural mitigation measures in reducing the failure probability of aboveground storage tanks (ASTs) were studied. Given past failures during flood and hurricane events, several studies have developed fragility models for ASTs. However, the suitability of these fragility models for different hurricane hazard scenarios is unknown. Furthermore, to combat climate change and sea level rise, several regional storm surge reduction strategies are being proposed. However, the effectiveness of these strategies in improving the safety of ASTs is also unknown. So, herein, a framework was proposed that facilitates assessing the suitability of fragility models and the quantification of AST failures and their consequences while propagating uncertainties using Monte Carlo simulations. The application of the proposed framework to Cameron, Louisiana, provided several key insights: (1) fragility models that do not model wave loads and dislocation failure are not suitable for the region; (2) a regional risk mitigation strategy was insufficient for lowering future spill volume, repair, and cleanup costs; and (3) considering bottom-plate failure of anchored tanks—a structural risk mitigation measure—would lead to a 47–72% reduction in the consequences of tank failure.

Keywords: aboveground storage tanks; hurricane; storm surge; fragility models; anchoring

check for updates

Citation: Ghimire, S.; Kameshwar, S. Assessing the Effectiveness of Regional Storm Surge Reduction Strategies and Tank Level Structural Mitigation Measures for Aboveground Storage Tanks. *J. Mar. Sci. Eng.* **2024**, *12*, 401. https://doi.org/10.3390/jmse12030401

Academic Editor: Markes E. Johnson

Received: 15 January 2024
Revised: 15 February 2024
Accepted: 22 February 2024
Published: 26 February 2024

Copyright: © 2024 by the authors. Licensee MDPI, Basel, Switzerland. This article is an open access article distributed under the terms and conditions of the Creative Commons Attribution (CC BY) license (https://creativecommons.org/licenses/by/4.0/).

1. Introduction

Aboveground storage tanks (ASTs) are a key component of petrochemical facilities, but they are vulnerable to damage during hurricane and flood events, which can have catastrophic consequences [1–3]. Investigations of past NaTech (technological accidents triggered by natural hazards) events during floods and hurricanes have also identified aboveground storage tanks (ASTs) as some of the most vulnerable equipment [4], which is the focus of this study. The risk to ASTs during floods and hurricanes is further compounded by the changing climate, which is expected to adversely affect the frequency and intensity of these natural hazard events [5,6]. Considering the potential consequences of AST failure, such as spills and ensuing damage to the surrounding environment [7,8] and communities [9–11], regional and tank-level mitigation strategies need to be developed and assessed for their effectiveness to ensure ASTs' safety for future climate conditions.

To facilitate vulnerability assessments of ASTs, several fragility models have been developed for ASTs that can estimate the probability of AST failure for given hazard conditions. There have been studies on AST performance during seismic hazards at the individual tank level [12–17] and at the regional level for a portfolio of tanks [18,19]. These studies mainly deal with tank responses to the sloshing of tank content and failure due to the buckling of tank shells and/or the failure of anchor chairs. For storm surges and hurricanes, Landucci et al. [20] first studied the vulnerability of ASTs based on a mechanical buckling damage model. Antonioni et al. [21] used this model to quantitatively assess the flood risk of AST facilities. Khakzad and Van Gelder [22,23] developed fragility functions

based on logistic regression and used a Bayesian network to merge the functions for buckling, floatation, and sliding failure modes. Kameshwar and Padgett [24,25] developed parameterized fragility models for floatation and buckling failure modes for ASTs for anchored and unanchored tanks based on logistic regression (LR). Yang et al. [26] developed parameterized fragility models based on LR for flood displacement, buckling failure modes, and combined displacement and buckling failure assuming them to be independent of each other. Some studies have included the effect of multiple hazards, such as wind, flood, rainfall, and/or waves, in the assessment of AST performance [27–31]. Bernier and Padgett [28] investigated the effect of waves on the buckling behavior of ASTs in conjunction with storm surges and concluded that static analysis is effective in estimating critical buckling load. Mayorga et al. [27] provided limit state equations for tank failures due to earthquakes, floods, and wind hazards separately. The effect of tank arrays on their vulnerability was also studied. Lan et al. [30] used multivariate joint distribution and fragility functions to study the dependence of hurricane floods and winds in calculating the failure probability of ASTs. Qin et al. [31] studied the floatation, sliding, wind buckling, flood buckling, and roof sinking failure modes of ASTs and employed a Bayesian network to assess tank vulnerability. Huang et al. [29] studied the coupling effect of floods and hurricanes in comparison with the direct superposition effect and found that the coupling effect significantly increases the vulnerability of ASTs. Mia and Kameshwar [32] studied the bottom plate failure in unanchored and anchored tanks and developed their fragility functions. Material failure in bottom plates and shells in tanks exposed to static flood waters was studied by Mia and Kameshwar [33], which revealed that anchoring tanks can lead to bottom-plate failure before shell buckling.

The abovementioned studies primarily focused on assessing the failure of individual ASTs. Limited studies have focused on assessing the performance of a regional portfolio of ASTs. To the best of the authors' knowledge, at present, there are only two studies that have assessed the performance of ASTs at the regional scale [34,35]. Kameshwar and Padgett [34] evaluated the performance of ASTs in the Houston Ship Channel region for two hypothetical hurricane storm surge scenarios. They developed estimates for repair costs, spill volumes, and downtime estimates for unanchored tanks. Furthermore, to reduce the impacts of AST failure, they suggested anchoring ASTs and compared the influence of anchorage on ASTs for the two synthetic storm surge scenarios and found that anchoring can reduce spill volumes by 40%. Similarly, for ASTs in the Houston Ship Channel region, Bernier et al. [35] explored engineering- and social-science-based approaches to select an optimum approach to reduce the effect of storm surges on petrochemical facilities and nearby communities. From the engineering perspective, they explored anchoring and filling up ASTs during hurricanes, which is not always feasible.

The above discussion highlights that there are several fragility models for assessing the performance of ASTs at the tank and regional levels for surge and flood hazards. At the regional level, limited studies have assessed the vulnerability of ASTs, and the effects of climate change on the performance of ASTs in a particular region have not been studied. Furthermore, for regional-level vulnerability assessment, there is a lack of understanding of the suitability of different fragility models for various hazard situations. An improved understanding of the suitability of different fragility models would facilitate informed vulnerability assessment and mitigation planning to improve the safety of ASTs. In this context, several regional-level mitigation measures for hurricanes and sea level rise have been proposed, which do not always explicitly consider ASTs. Nevertheless, the effectiveness of such regional-level mitigation strategies for reducing the failure of ASTs for current and future conditions needs to be assessed, as it is not known. Furthermore, for individual ASTs, anchoring has been suggested as a structural mitigation measure. However, the effectiveness of anchoring ASTs as a mitigation measure for individual tanks in light of new fragility models, such as bottom-plate failure fragility models [32,33], has not been assessed for a regional portfolio of ASTs. Considering these gaps, the objective of this research was to assess the effectiveness of regional storm surge reduction strategies and

tank-level structural mitigation measures in reducing the failure probability of ASTs and understand the suitability of different fragility models for regional application. This study was conducted for a number of tanks at a particular location for a given hurricane, and multiple similar scenarios were analyzed; however, the probability of a hurricane in itself was not considered. To compare different measures, failure probabilities, spill volumes, and repair costs were used herein, which were quantified using a general framework.

The latter part of this paper includes the following sections. Section 2 describes the steps involved in the proposed framework for the probabilistic performance assessment of ASTs. Section 3 demonstrates the use of the framework to select suitable fragility models based on tank failures observed during Hurricane Laura in August 2020. In Section 4, a case study of Cameron Parish, Louisiana, is presented, where the effectiveness of the 2023 Louisiana Coastal Master Plan (CMP) [36], a regional hurricane risk reduction strategy, was assessed. The effectiveness of anchoring as a structural mitigation measure for individual tanks was also studied for various hazard scenarios in Section 5. The conclusions and future works based on this research are presented in Section 6.

2. Methodology

Herein, a general framework for the assessment of AST failure probabilities, the consequences of failures, and an evaluation of mitigation measures is proposed. Each step is shown in a flowchart in Figure 1, and the overall procedure is described in the subsequent five subsections.

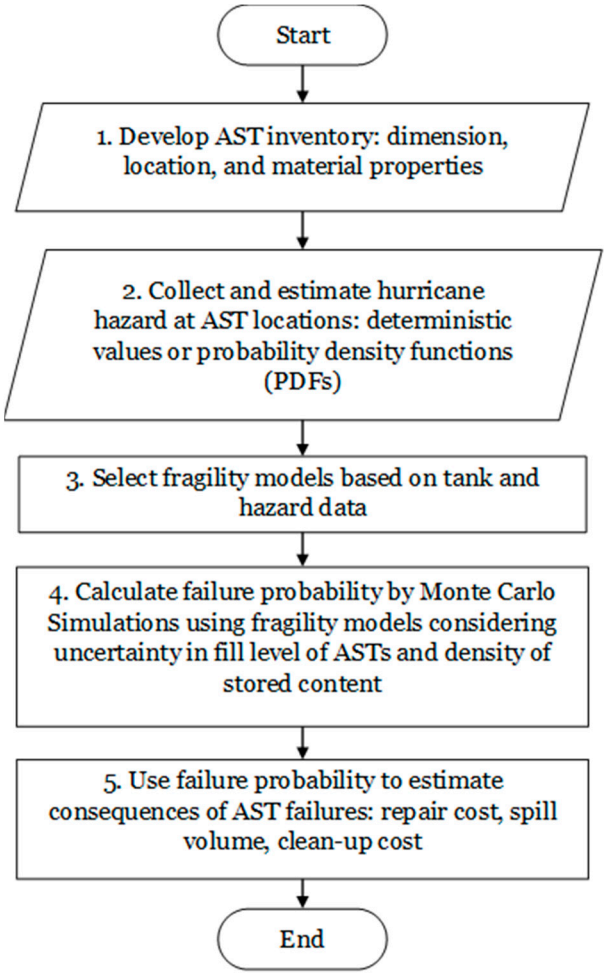

Figure 1. Flowchart of regional vulnerability assessment framework.

2.1. Developing Inventory of ASTs (Step 1)

The first stage is the development of an AST dataset containing the location, size, and content of ASTs for a particular region. If there is a lack of publicly accessible data, a new dataset needs to be created. Satellite and aerial images can be used to locate the tanks and measure their diameters. The tank roof type (fixed or floating) can be identified utilizing these images. A digital elevation model (DEM) and a digital surface model (DSM) can be used to measure tank heights. A DEM is a bare-earth elevation model that excludes all surface objects, whereas a DSM includes the elevations of all the surface objects. Thus, a DEM can provide ground elevation at an AST's location, and a DSM can provide the elevation of the roof of an AST. So, the difference in elevation between the DSM and DEM at the location of a tank can be taken as the height of the tank.

2.2. Hazard Estimation (Step 2)

At each AST location, storm surge inundation depth, maximum wind velocity, current velocity, and significant wave height are required to assess the probability of failure using fragility models. The past hurricane hazard data for the US Atlantic and Gulf Coast can be obtained from several sources, such as the National Oceanic and Atmospheric Agency (NOAA) [37] and the Coastal Emergency Risk Assessment (CERA) website [38]. Alternatively, hazard data for various return periods can be obtained from simulation-based estimates [39–41]. All of these hazard intensity measures, mentioned in Table 1, can be deterministic values or be described by probability distributions depending on the uncertainty of the data.

Ideally, the probabilistic approach should be preferred because it includes uncertainties in the analysis; however, in the absence of actual probabilistic data, probability models for various parameters used in past analyses can also be used. Parameters can be used deterministically if the resultant effect due to uncertainty is found to be insignificant. On the other hand, parameters such as the height of the content inside the tank and the density of stored content are always used with probability distributions as the resultant effect is found to be sensitive to these parameters.

2.3. Fragility Models Selection (Step 3)

Fragility models are conditional probability models that describe the probability of exceeding different limit states (such as buckling, floatation, sliding, system failure, and bottom-plate failure for ASTs) for a given hazard (storm surges, wind, and waves) and tank parameters (height, diameter, fill level, liquid density). Existing studies have developed fragility models for storm surge floatation [20,21,25], storm surge sliding [22,23], storm surge dislocation [26,27], storm surge buckling [25–27], wind buckling [27,34], system failure [22,23,28,31], and bottom-plate failure [32] during storm surges. Fragility models for AST failures have been developed using probabilistic methods to quantify the probability of AST failure as a function of tank and hazard parameters. Logistic regression, Bayesian networks, and Monte Carlo simulation are the commonly used statistical inference techniques used to develop these fragility models. Furthermore, different modes of structural failures have been studied using finite element analysis (FEA) or analytical equations to assess the effect of different loads and boundary conditions. Depending on the expected hazards and the objective of the analysis, appropriate fragility models should be selected.

2.4. Failure Probability Calculation (Step 4)

Using a fragility model parameterized on tank parameters (X) and intensity measures (IM), the probability of failure for a given failure mode can be determined considering uncertainties in random parameters using Equation (1):

$$P\left[Failure\right] = \int_X \int_{IM} P\left(Failure \,|X, IM\right) f_X(X) f_{IM}(IM) \mathrm{d}X \, \mathrm{d}IM \tag{1}$$

Here, P ($Failure \mid X, IM$) is a fragility model for a given mode of failure conditioned on tank parameters (X) and intensity measures (IM); $f_X(X)$ and $f_{IM}(IM)$ are the joint probability density functions (PDFs) of X and IM, respectively. Variables that are included in X and IM are given in Table 1. The multi-dimensional integration requires the joint probability distribution of the parameters, which can be difficult to obtain. Hence, variables can be assumed to be independent, and their joint PDF can be obtained by multiplying their marginal PDFs. Fragility models can be selected from the abovementioned models to calculate failure probability based on the tank and hazard data available. The overall failure probability, considering all failure modes, can also be evaluated using a series system assumption [42]. Equation (1) can be evaluated using Monte Carlo simulations (MCSs), as presented in Figure 2, to account for the uncertainty associated with the random variables. For this purpose, Latin hypercube sampling (LHS) or other efficient sampling methods [43,44] can be used to reduce the number of simulations required to obtain the probability of failure.

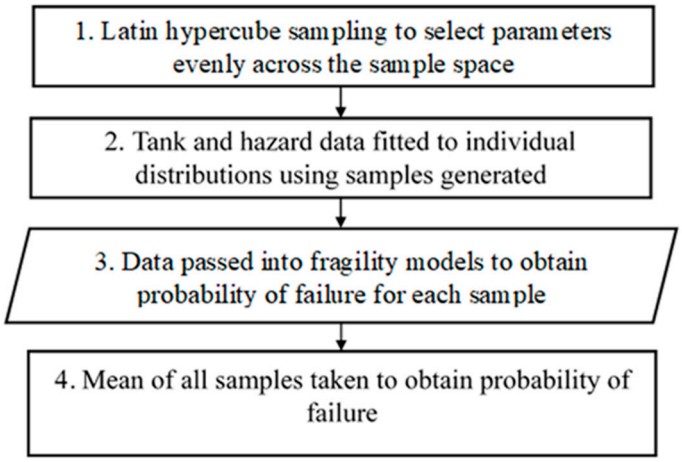

Figure 2. Algorithm showing Monte Carlo simulation used in this analysis.

2.5. Consequence Modeling (Step 5)

Financial costs for loss of liquid content, repair needs for tanks, the cleanup of spilled liquid, disruptions in the supply chain, and litigation can be quantified based on previous studies and experiences. However, the undeniable environmental and social costs of potential spills could be far worse. However, the quantification of these indirect costs is beyond the scope of this research. This study only includes the consequences of AST failures such as spill volume, repair cost, and cleanup cost using fragility models. Equation (2) estimates the expected spill volume assuming that a failure leads to the spillage of the entire contents of the tank.

$$E[Spill\ volume] = \int_X \int_{IM} \frac{\pi L D^2}{4} P\ (Failure \mid X, IM) f_X(X) f_{IM}(IM) \mathrm{d}X\ \mathrm{d}IM \quad (2)$$

where L (included in X) is the height of the stored contents of the tank, and ($\pi LD^2/4$) is the volume of the stored contents. The above spill volume estimate also depends on the density of the stored contents, ρ, which is included in IM. The distributions of L and ρ are given in Table 1. The above equation propagates the uncertainties of uncertain parameters such as fill level and liquid density to assess the spill volume. Using the spill estimates, the cleanup costs can be determined from existing studies [35,45–48]. Etkin [47] provides a comprehensive cleanup cost estimation model based on the location of the spill (continent and country and distance from shore), oil type, cleanup strategy, and spill volume. These costs can be converted into present-day costs by adjusting for inflation using annual inflation rates provided by the US Bureau of Labor Statistics [49].

Using the approach used for estimating spill volume, the expected repair cost of ASTs can be calculated using damage ratios following Equation (3):

$$E\left[Repair\ cost\right] = Cost \times inflation \int_r \int_X \int_{IM} r \cdot P\left(Failure\,|X, IM\right) f_X(X) f_{IM}(IM) f_r(r) \mathrm{d}X\ \mathrm{d}IM \mathrm{d}r \quad (3)$$

where $f_r(r)$ is the PDF of the damage ratio [34], which is the ratio of the repair cost to the total cost of the tank. The cost of a new tank (*Cost*) can be obtained via interpolation or extrapolation for a given volume of tank based on the Michigan Tax Assessor's Manual [50]. Furthermore, *Cost* can be adjusted for inflation using inflation rates provided by the US Bureau of Labor Statistics [49].

Table 1. Tank parameters and hazard data with their distributions.

Parameter (Unit)	Symbol	Distribution	References
Diameter (m)	D	Deterministic	–
Height (m)	H	Deterministic	–
Storm surge (m)	S	Deterministic, lognormal	–
Maximum wind velocity (m/s)	V	Deterministic	–
Product design stress (MPa)	S_d	Deterministic, uniform	[51]
Significant wave height (m)	H_s	Deterministic	–
Individual wave height in a group of waves(m)	H_w	Weibull probability distribution	[52]
Current velocity (m/s)	U	Uniform (0.2)	[53]
Coefficient of friction	Φ	Uniform (0.3–0.7)	[53]
Liquid height in tank (m)	L	Uniform (0, 0.9H)	[25]
Specific gravity of liquid	ρ	Uniform (0.5, 1) for petroleum fluids; uniform (1.8, 2.4) for drilling fluids	[25]
Damage ratio	r	Uniform (0.8–1) for storm surge floatation	[34]
Thickness of bottom plate (m)	t	Deterministic	–
Yield strength of bottom plate (MPa)	F_y	Deterministic	–

3. Assessing Suitability of Existing Fragility Models

This section demonstrates the use of the proposed framework to determine the suitability of various fragility models for a case study region. Understanding the suitability of fragility models is essential for regional-level applications to ensure the reliability of estimates on tank failures and spill volumes. To this end, this section aims to determine the suitability of various fragility functions for a case study region—Cameron Parish, Louisiana. It was selected, herein, because of AST failures observed during Hurricane Laura in 2020. The critical factor considered to determine the effectiveness of a fragility model was its ability to accurately predict failed and unaffected ASTs during Hurricane Laura. Figure 3a shows the Gulf Coast region of the US, the path of Hurricane Laura, and the location of Cameron Parish in Louisiana. Following the framework described in the previous section, an AST inventory was created using Google Earth Pro [54] with satellite images that helped to locate and measure the diameters of ASTs in Cameron Parish. The roof types were also identified utilizing aerial images. Furthermore, NOAA Hurricane Laura imagery [55] was used to identify AST failures due to the hurricane. The locations of unaffected and failed ASTs during Hurricane Laura in August 2020 in Cameron Parish (Louisiana) are shown in Figure 3b.



(**a**)

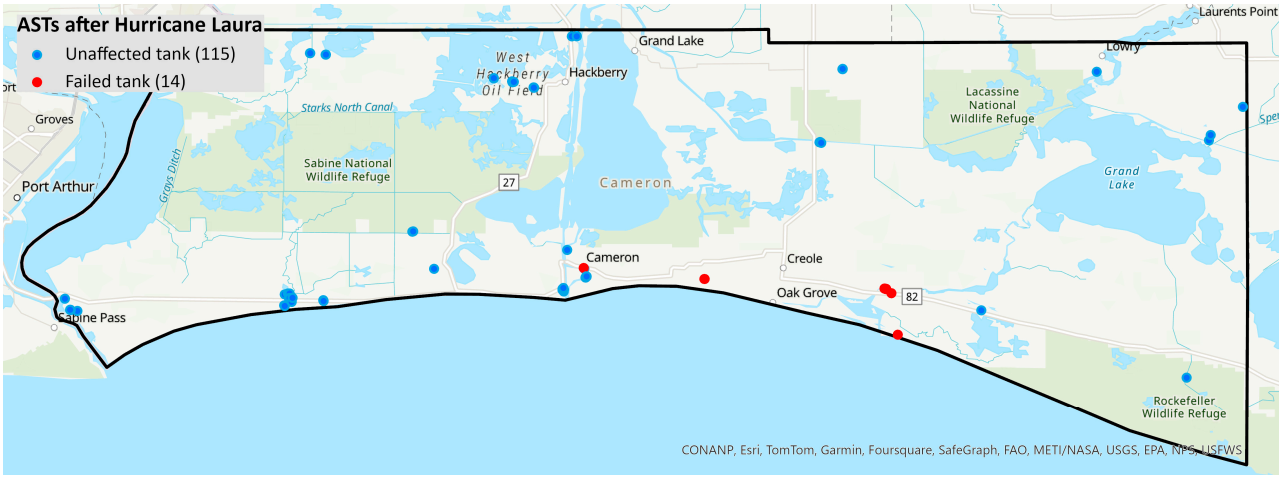

(**b**)

Figure 3. (**a**) Hurricane Laura's path and Cameron Parish. (**b**) Failed and unaffected ASTs after Hurricane Laura in Cameron Parish, Louisiana.

ArcGIS Pro 3.2 [56] was used to create digital elevation and surface models using 2017 USGS Lidar point cloud data for the Chenier Plain in Louisiana [57]. These DSMs and DEMs were further used to calculate the heights of ASTs following the process mentioned in the Methodology section. Data on maximum wind speed, inundation depth above the ground level, and significant wave height during Hurricane Laura were obtained from the Coastal Emergency Risk Assessment (CERA) [38] website. Using these data, raster images were created, and values of the hazard intensity measures were determined at each AST location employing ArcGIS Pro. Individual tanks or entire tank farms are often surrounded by containment dikes to confine spills. In Cameron Parish, the water depth was at times over 10 feet, at which point, these containment dikes would be overtopped. Therefore, the height of these dikes was not considered in this study. Otherwise, a cut-off surge height based on the height of levees should be used. The Coastal Engineering Manual [58] was used to convert the mile-per-hour windspeed to a 3 s gust windspeed for later use in system and dislocation fragility models. Furthermore, utilizing the significant wave height estimate, 3 s gust windspeed, and water depth, the shallow water wave height estimates were probabilistically generated using the general Weibull probability distribution [52].

Additionally, the wave period (T_w) was calculated based on ASCE 7-22 Supplement 2 [59], provided in Equation (4).

$$T_w = 12.1\sqrt{\frac{H_w}{g}} \tag{4}$$

where H_w is the individual wave height in an ensemble of waves, and g is the acceleration due to gravity.

To understand the performance of storage tanks during Hurricane Laura, 1000 Monte Carlo simulations (MCSs) were performed to predict AST failures considering uncertainties in the fill level of ASTs and the density of stored contents. One thousand MCS were chosen after performing convergence analysis where the number of samples were changed and the probability of failure could be observed. Based on this analysis, 1000 samples were found to be sufficient. Employing these, the probabilities of failure for unanchored ASTs were calculated employing existing fragility models for storm surge floatation [25], storm surge buckling [25], wind buckling [34], system failure [53], and dislocation [53]. Among the different fragility models available in the literature, these models were selected because these models were parameterized based on tank parameters, which makes them suitable for application to a regional portfolio of ASTs. The prediction of the number of AST failures based on the different fragility models is shown in Table 2. Herein, a tank was considered to fail if the average of 1000 probabilities of failure obtained from all MCSs exceeded 0.5. A probability of failure greater than 0.5 is taken as a failure, which is a notional idea of failure, and the binary output (failed or not failed) is useful in decision making. Here, F_a is the set of tanks that actually failed during the hurricane, which is equal to 15, and F_p is the set of tanks predicted to fail using fragility models.

Table 2. F_a and F_p values for different failure modes.

Limit States	F_p	$F_p \cap F_a$	$F_p - F_a$	$F_a - F_p$
Storm surge floatation [25]	46	10	36	5
Storm surge buckling [25]	1	1	0	14
Wind buckling [34]	0	0	0	15
System (floatation, buckling, and sliding) failure [53]	51	13	38	2
Dislocation (sliding and floatation) failure [53]	51	13	38	2

Here, system failure and dislocation fragility models captured most of the tank failures during Hurricane Laura effectively, as both of them predicted 13 out of 15 failures. System and dislocation failure models also included wave loads in the failure prediction and were able to better identify the failed tanks. This observation indicates that there were significant wave-induced loads on tanks in Cameron during Hurricane Laura. Therefore, fragility functions, which include wave-induced forces, should be considered for future assessments of ASTs in Cameron Parish, LA, and other coastal regions with significant wave action during hurricanes. Consequently, herein, system failure and dislocation fragility models for unanchored ASTs subjected to concurrent surges, waves, and wind were used to estimate the probability of failure using parameterized fragility functions [53]. The probability of failure for tanks due to system and dislocation failures in ASTs can be provided by Equation (5).

$$P\,(Failure) = \int_L \int_\rho P\,(Failure\,|D,\ H,\ l,\ S_d,\ S,\ \rho,\ V,\ H_w,\ t_w,\ U,\ \Phi) f_{T_w}(t_w) f_L(l) f_\rho(\rho)\ dl\ d\rho \quad (5)$$

Here, parameters and their distributions are described in Table 1. S_d is product design stress, which is dependent on F_y.

On the other hand, the floatation fragility model overestimated tank failures by 36, and the system failure and dislocation fragility models overestimated tank failures ($F_p - F_a$) by 38. The overestimation by these models could be explained by the following reasons:

1. A large number of tanks that were expected to fail but did not actually fail were in clusters of 13 in one place and 15 in another place. A few small diameter tanks (<5 m) located within the cluster of 13 tanks failed. Moreover, two separate tanks

(not in a group) very close to these tanks also failed. Tanks behind the first line of tanks experienced shielding and/or channeling effects from wave action. These observations indicate group effects, which are not considered in existing fragility models that can be applied to a portfolio of regional ASTs.

2. Pipe connections between tanks and processing facilities could have prevented AST failures. There have been studies on stress on shell–pipe connections due to seismic loading [60,61] and tank settlement [62]. Stresses develop in the tank shell because of the differential settlement of the tank in relation to the pipe or pipe rack system [21]. Fragility curves are slightly different if the coupling of pipes and tanks is not included in the analysis [63]. Hence, it can also be inferred that stresses developing in the tank shell at the pipe–shell junction could provide a downward reaction opposing the uplift force of the tank. However, the exact quantification of stress due to tank uplift needs further study.
3. The tank failure depends on the level of fill in the tank. A higher level of fill reduces the probability of failure and vice versa. Herein, the fill level was assumed to follow a uniform distribution. It is plausible that the tanks might have had a high fill level, which might have prevented their failure.

Few studies have assessed the impact of group effects on the failure of ASTs [27], but the existing studies are limited in their applicability to large groups of ASTs, such as the ones observed in Cameron Parish. Furthermore, the system and dislocation fragility model could not capture two tank failures ($F_a - F_p$). The reasons might be uncertainty in the fill level of the ASTs or debris impact, which are both hard to quantify. However, the probabilities of failures for these tanks were 0.46 and 0.47 for both system and dislocation failures, which are very close to 0.5. This section provides a demonstration of how to determine suitable fragility models for regional-level vulnerability assessments of ASTs exposed to floods and storm surges. The following section will apply the framework to a case study region to assess this vulnerability for current and future scenarios.

4. Effectiveness of Regional-Level Risk Mitigation Measures

The 2023 Coastal Master Plan (CMP) prepared by the Louisiana Coastal Protection and Restoration Authority (CPRA) details issues southern Louisiana faces at present because of land loss, storm-surge-based flooding risk, and future sea level conditions [36]. In the master plan, future coastal landscapes are projected, along with how land use decisions, subsidence, and climate change may affect where and how coastal regions can prosper. In Cameron Parish, CMP projects include large-scale marsh development and hydrologic restoration (creating drainage infrastructure or expanding the capabilities of existing structures). Furthermore, Cameron Parish is home to an abundance of animals and marshlands; the oil spills resulting from AST failures will harm the ecosystem. Moreover, cleanup efforts are expensive and harm a variety of habitats, species, and ecological processes [64]. However, no levee construction projects or other structural risk reduction initiatives have been proposed for this region. Therefore, the effectiveness of the existing mitigation measures proposed in the CMP for preventing the failure of ASTs in Cameron Parish was first evaluated in this study.

A life cycle analysis could be relevant to this study. However, based on available data and the objective of this study, that is, to analyze the effectiveness of the Coastal Master Plan for ASTs, a comparison of two CMP scenarios is presented in this study. Since only one variable is changed (mitigation measure) in these analyses, these observations provide several insights into the effectiveness of these strategies at various hazard levels, which can be used by stakeholders to select mitigation measures.

4.1. Tank Inventory and Hazard Estimation

The tank inventory of Cameron Parish used in the validation was used for this case study. For hazard data, the results from the ADCIRC hurricane simulations [36] conducted to inform the CMP considering different mitigation measures and future sea level and

subsidence conditions were used. The hazard data consist of storm surge inundation depths for more than 110 thousand grid points for three cases: present, future without action (FWOA), and future with master plan (FWMP). The FWOA condition in the 2023 Coastal Master Plan serves as the baseline for predicting changes in the landscape and storm-surge-based risk in the future. The FWMP condition considers the future landscape of coastal Louisiana with the full implementation of the 2023 CMP. Both FWOA and FWMP cases include future storm surge data for three landscape scenarios (low, medium, and high), three future years (2025, 2040, and 2065), and five return periods (10, 50, 100, 250, and 500 years) at each grid point. Furthermore, the inundation data include 10th, 50th, and 90th percentile values. However, the present case only considers the year 2015 for different return periods and percentile values. Thus, there are 285 cases of storm surge inundation data. Using this data, flood depth raster images were created for all FWOA, FWMP, and present cases using Ordinary Kriging in ArcGIS Pro 3.2 [56]. The flood depth values at all AST locations were obtained at 10th, 50th, and 90th percentile values using these raster images. These percentile values were used to fit lognormal distributions to the inundation depth, which was used in the MCS.

4.2. Fragility Model Selection

Section 3 identified dislocation and system fragilities as the most appropriate for the case study region. However, to apply these fragility models, wave hazard information is necessary, which was not available in the Coastal Master Plan data for future and present conditions. Given the unavailability of this data, a fragility model for storm surge floatation [25] for unanchored tanks, which is the second-best fragility model, was used. Furthermore, the main objective of the hazard data is to compare the failure probability and consequences of failure with or without the Coastal Master Plan so that the analysis can be used for the improvement of the next Coastal Master Plan. All ASTs were considered to have fixed roofs since ASTs in the area were identified as fixed-roof tanks using satellite imagery. Finally, anchoring is not generally practiced in the study area, so tanks were assumed to be unanchored.

4.3. Failure Probability Calculation

The lognormal distribution fit to inundation depths at each tank's location was used to sample inundation depths at each AST location. Furthermore, the inundation depths at AST locations were correlated to ensure that inundation depths at different AST locations were meaningful and followed the local topography. Using this approach and the selected fragility model, 1000 Monte Carlo simulations were performed to estimate AST failures considering uncertainties in the fill level of ASTs and the density of stored contents. The average of the failure probability values from all simulations of a tank was considered its failure probability.

4.4. Consequence Modeling

The procedure mentioned in the Methodology section was used to calculate spill volumes, cleanup costs, and repair costs for storm surge floatation failure in unanchored tanks for all cases. Herein, cleanup costs of USD 12/L (in 2006 USD) were used based on Bernier et al. [35] and were adjusted for inflation using annual inflation rates provided by the US Bureau of Labor Statistics [49]. For repair costs, the damage ratio was obtained from Kameshwar and Padgett [34] along with estimates of the cost of a new tank obtained from the Michigan Tax Assessor's Manual [50]. The repair costs were also adjusted for inflation. The average of consequences of all simulations for a tank was considered its consequence.

4.5. Comparison of Results for FWOA and FWMP

Figure 4a,b compare the failure probability of ASTs in Cameron Parish for FWOA and FWMP cases considering a 100-year-return-period-hurricane-induced surge hazard in the year 2040 for a medium sea level rise scenario. Other combinations of return periods and

sea level rise scenarios are not shown for brevity. The center of a circle shows the location of a tank, and a larger diameter circle represents a higher probability of failure. Furthermore, the color and size of the circles correspond to the range of failure probability shown in the legend. The comparison of failure probabilities and number of tank failures between FWOA and FWMP cases does not show significant improvement.

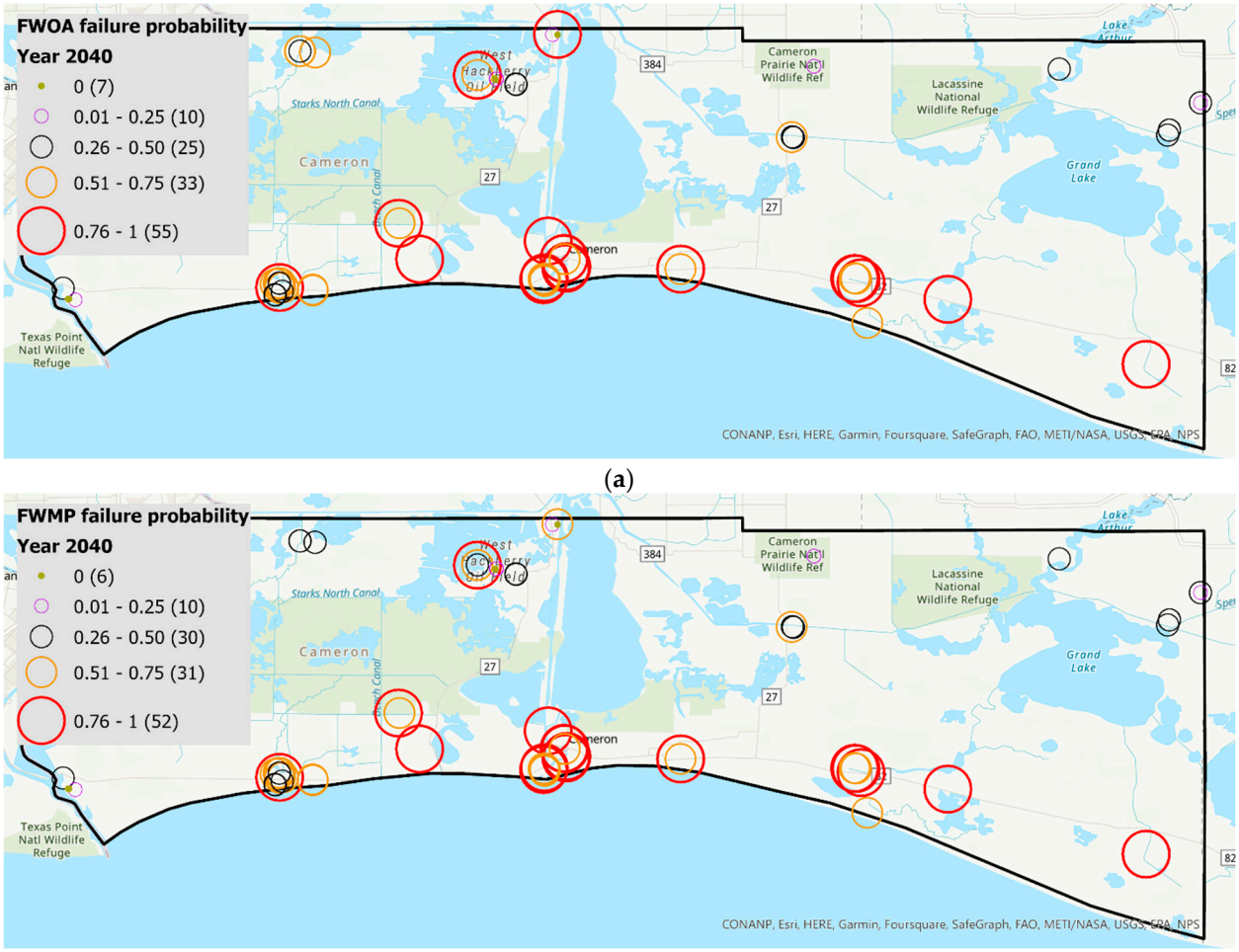

Figure 4. Medium scenario, 100–year return period in the year 2040. (**a**) FWOA failure probability; (**b**) FWMP failure probability.

For other future years and return periods, Table 3 shows a comparison of expected spill volumes for all tanks during storm surge events due to tank failure for all present scenarios and medium scenarios in FWOA and FWMP using 1000 Monte Carlo simulations. Spill volumes for FWOA and FWMP cases are comparable with a less than 10% difference. To understand the variability in the spill volumes reported in Table 3, Table 4 shows the coefficient of variation among spill volumes and cleanup costs. As cleanup cost was directly proportional to spill volume, the coefficients of variation are the same for each case of spill volume and cleanup cost. A comparison of coefficients of variation from FWOA and FWMP shows minor differences. Furthermore, the coefficients of variation are low (about 0.2) for return periods greater than 100 years. This observation indicates that there is low uncertainty around the spill volume estimates, which can be used for decision making regarding the selection of mitigation measures.

Table 3. Spill volume for present and future conditions (m^3).

Present Scenario					
Year	Return Period in Years				
	10	50	100	250	500
2015	733	3770	6546	8209	9728
FWOA Medium Scenario					
Years	Return Period in Years				
	10	50	100	250	500
2025	0	3733	7405	9506	10,312
2040	0	4678	8553	10,419	11,163
2065	0	7433	11,176	13,246	13,900
FWMP Medium Scenario					
Years	Return Period in Years				
	10	50	100	250	500
2025	0	4154	7322	9253	9803
2040	0	4808	8167	9767	10,262
2065	0	7094	10,077	11,718	12,155

Table 4. Coefficient of variation of spill volume and cleanup cost.

Present Scenario					
Year	Return Periods in Years				
	10	50	100	250	500
2015	1.15	0.45	0.30	0.28	0.36
FWOA Medium Scenario					
Years	Return Period in Years				
	10	50	100	250	500
2025	3.52	0.48	0.27	0.24	0.21
2040	3.52	0.42	0.26	0.23	0.20
2065	3.52	0.34	0.22	0.20	0.18
FWMP Medium Scenario					
Years	Return Period in Years				
	10	50	100	250	500
2025	2.36	0.42	0.24	0.21	0.17
2040	2.36	0.37	0.23	0.18	0.16
2065	2.36	0.30	0.18	0.15	0.13

Figure 5 shows the expected spill volume for each tank for a medium scenario, 100-year return period in the year 2040 for the FWMP case. The number of tanks within each of the given ranges is also shown in the legend. Cleanup costs are not shown here since they are directly proportional to the spill volumes. Spill volumes for the FWOA case were also calculated but are not shown here because of a lack of significant differences. A comparison of Figure 5 with Figure 4b shows that a high probability of failure does not necessarily correlate well with a high spill volume, which could be attributed to the size of the ASTs. High spill volumes are caused by large ASTs with high failure probabilities.

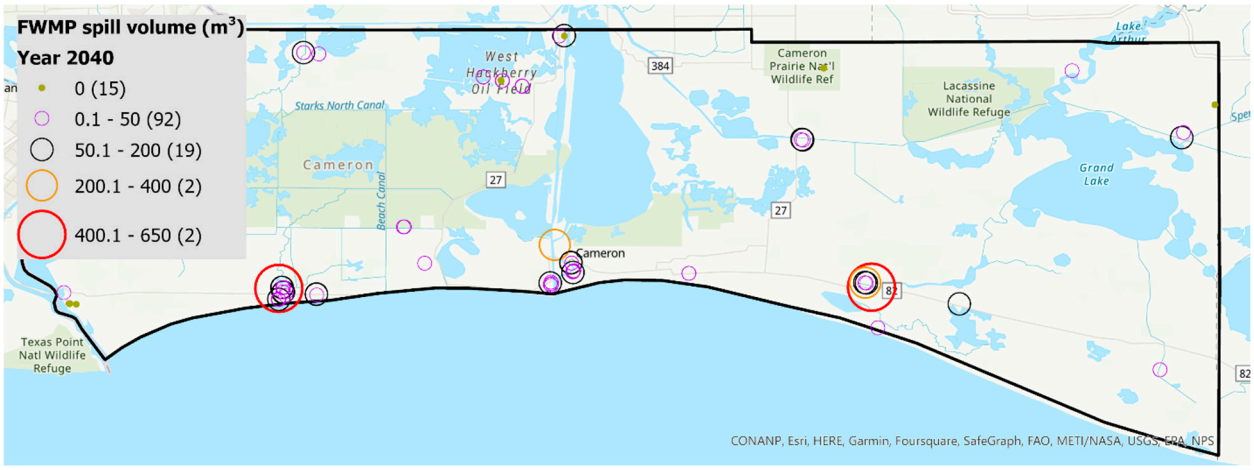

Figure 5. Spill volumes for FWMP (medium scenario, 100–year return period in the year 2040).

Table 5 shows a comparison of expected repair costs for all tanks during storm surge events due to tank failure for all present scenarios and medium scenarios in the FWOA and FWMP cases. The coefficient of variation had minor differences in the FWOA and FWMP cases, which are not shown here for brevity. Figure 6 shows the expected repair costs of each tank in a medium scenario, 100-year return period in the year 2040 for the FWMP case, which is similar to that of the corresponding FWOA case.

Table 5. Repair Cost (USD).

Present Scenario					
Year	Return Periods in Years				
	10	50	100	250	500
2015	1,232,788	9,933,530	17,666,069	21,989,385	25,768,207
FWOA Medium Scenario					
Years	Return Periods in Years				
	10	50	100	250	500
2025	46	10,699,171	19,726,020	24,203,285	25,632,010
2040	46	12,719,807	22,1483,31	25,764,133	27,110,060
2065	46	19,081,387	26,965,001	30,107,692	31,040,392
FWMP Medium Scenario					
Years	Return Periods in Years				
	10	50	100	250	500
2025	46	11,052,917	19,486,645	24,095,399	25,433,490
2040	46	12,709,274	21,719,007	25,624,617	26,756,625
2065	46	18,953,796	26,615,146	29,833,792	30,930,768

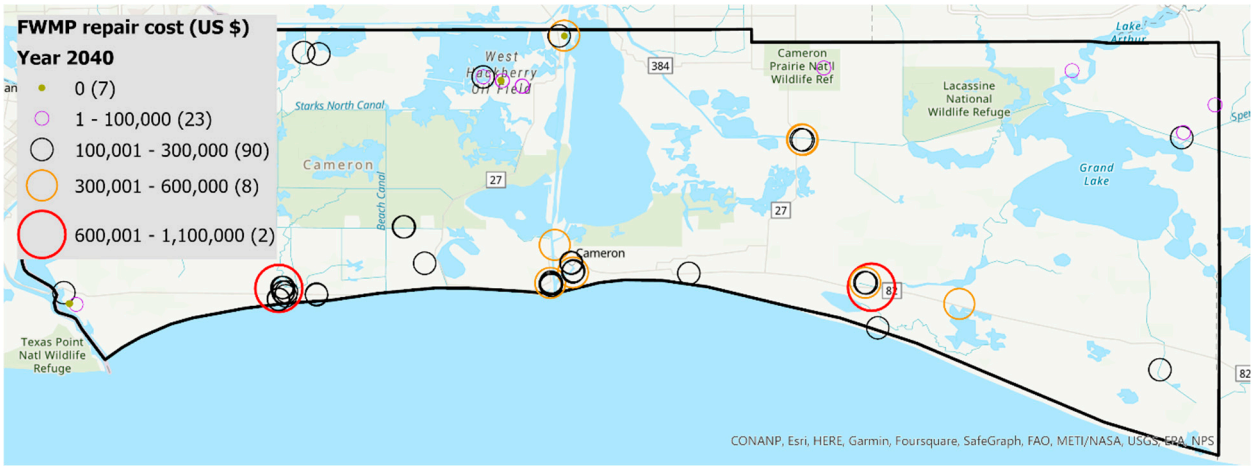

Figure 6. FWMP repair cost (medium scenario, 100–year return period in the year 2040).

Figures 1–5 and Tables 3–5 illustrate that the probability of AST failures and the consequences of AST failures would not change by a significant amount because of the implementation of the Master Plan. This observation is partly expected since the mitigation of AST failures is not considered in the Coastal Master Plan. Furthermore, the hurricane-induced failures and the subsequent consequences of AST failures would also increase in subsequent years. Some tanks with a greater probability of failure do not necessarily have greater consequences of failure (spill volume, cleanup cost, repair cost) because consequences of failure also depend on the volume of the tank: the larger the tank volume, the greater the consequences. Hence, the current regional risk mitigation strategy needs to be improved, and structural mitigation strategies should also be employed at the level of individual ASTs to improve their performance during hurricanes in the future.

5. Effectiveness of Structural Mitigation Measures for Individual Tanks

Since the regional-level hurricane risk mitigation strategy for the case study area is not effective, tank-level mitigation measures were considered herein. Anchoring tanks to the ground to prevent flotation and sliding failures has been recommended as a structural mitigation measure. Kameshwar and Padgett [34] studied the use of anchors to prevent tank failure due to storm surge floatation in the Houston Ship Channel and concluded that anchoring could reduce expected repair costs and spill volumes by 40%. However, recent studies [32] have indicated that anchored tanks' bottom plates might yield or rupture during storm surge events because of buoyancy-induced uplift pressure. The fragility models for bottom plate failure developed by Mia and Kameshwar [32] were used to calculate the probability of bottom-plate failure as per the procedure in the Methodology section.

Table 6 shows the percentage reduction in expected spill volumes due to anchoring for all present scenarios and medium scenarios for FWOA and FWMP cases using 1000 Monte Carlo simulations. The percentage reductions in spill volumes have minor differences between the FWOA and FWMP cases. The results show that the expected spill volume, repair cost, and cleanup cost will reduce significantly if the tanks are anchored. As shown in Table 6, anchoring tanks would lead to a 47–72% decrease in the consequences of AST failures except for 10-year return period cases. However, anchoring does not completely eliminate failures. Therefore, additional measures may be necessary to further reduce the failure probability and consequent spill volume of ASTs subjected to storm surges.

Table 6. Percentage reduction in mean spill volume and cleanup costs after anchoring ASTs.

Present Scenario					
Year	Return Periods in Years				
	10	50	100	250	500
2015	79	72	68	63	56
FWOA Medium Scenario					
Years	Return Periods in Years				
	10	50	100	250	500
2025	-	64	61	57	56
2040	-	65	60	57	56
2065	-	63	57	52	52
FWMP Medium Scenario					
Years	Return Periods in Years				
	10	50	100	250	500
2025	-	67	61	57	55
2040	-	67	59	55	53
2065	-	61	53	47	46

6. Conclusions

This study focused on assessing the effectiveness of regional storm surge reduction strategies and tank-level structural mitigation measures to reduce the failure probabilities of ASTs and understand the suitability of different fragility models for regional applications. For this purpose, a general framework for the estimation of aboveground storage tank (AST) failure probabilities and the quantification of the consequences of failure was proposed. First, the proposed framework was used to demonstrate the suitability of existing fragility models for the vulnerability assessment of a regional portfolio of ASTs in Cameron, LA, where tank failures were observed during Hurricane Laura in 2020. Additionally, the same approach was used to assess the effectiveness of Louisiana's Coastal Master Plan (a regional-scale hurricane risk mitigation plan) in reducing the probability of AST failures, potential spills, cleanup costs, and repair costs. Furthermore, the effectiveness of anchoring (a structural mitigation strategy for individual tanks) considering bottom-plate failures was also assessed using the proposed framework. The conclusions of this study are summarized below:

1. The application of the proposed framework to Cameron, LA, to assess the suitability of fragility models showed that storm surge floatation and dislocation were the main causes of AST failures during Hurricane Laura. However, the concurrent effect of storm surge, wave, and wind loads was also significant. Thus, it is essential to consider wave loads to estimate the failure probability of ASTs near the coast. Furthermore, if possible, group effects should also be considered.
2. The results indicate that the effects of storm surge inundation on ASTs are likely to increase in the future because of sea level rise. Thus, the AST infrastructure located in coastal Louisiana and the Gulf Coast of the US is at risk during such events.
3. The Louisiana Coastal Master Plan, a regional-level coastal risk mitigation measure, was found to be insufficient in reducing the failure probability of ASTs in Cameron, LA, for present and future conditions across various return period events. More projects need to be considered near ASTs for the regional-level mitigation of AST failures.
4. Anchoring ASTs during hurricane events could reduce the number of tank failures and their consequences. However, tanks might fail because of yielding or ruptured bottom plates, as they are subject to uplift forces, which are not considered in the

design of bottom plates. Hence, more tank-level structural level mitigation measures need to be developed.

Future work could include the assessment of group effects on the performance of tanks, the effects of pipes on the performance of ASTs, and the development of structural mitigation measures considering different failure modes including bottom-plate failure.

Author Contributions: Conceptualization, S.G. and S.K.; methodology, S.G. and S.K.; software, S.G. and S.K.; validation, S.G. and S.K.; formal analysis, S.G. and S.K.; investigation, S.G. and S.K.; resources, S.G. and S.K.; data curation, S.G. and S.K.; writing—original draft preparation, S.G.; writing—review and editing, S.G. and S.K.; visualization, S.G. and S.K.; supervision, S.K.; project administration, S.K.; funding acquisition, S.K. All authors have read and agreed to the published version of the manuscript.

Funding: This research was funded by Coastal Protection and Restoration Authority (CPRA) of Louisiana under Coastal Science and Assistantship Program (CSAP).

Institutional Review Board Statement: Not applicable.

Informed Consent Statement: Not applicable.

Data Availability Statement: The data presented in this study are available on request from the corresponding author.

Acknowledgments: The authors are thankful to the Coastal Protection and Restoration Authority (CPRA) for providing the storm surge data.

Conflicts of Interest: The authors declare no conflicts of interest. Any opinions, findings, conclusions, or recommendations expressed herein are those of the authors and do not necessarily reflect the views of the CPRA.

References

1. Godoy, L. Performance of Storage Tanks in Oil Facilities Damaged by Hurricanes Katrina and Rita. *J. Perform. Constr. Facil.* **2007**, *21*, 441–449. [CrossRef]
2. Murphy Oil Spill, Volume 2014, No. 11 August 2008. Available online: http://www.epa.gov/katrina/testresults/murphy/index.html (accessed on 27 December 2023).
3. Hyder, M. (Ed.) *Oil Spill Intelligence Report, Assessment of Hurricane Ike Damage Continues*; Aspen Publishers: New York, NY, USA, 2008.
4. Cozzani, V.; Campedel, M.; Renni, E.; Krausmann, E. Industrial accidents triggered by flood events: Analysis of past accidents. *J. Hazard. Mater.* **2010**, *175*, 501–509. [CrossRef]
5. Mudd, L.; Wang, Y.; Letchford, C.; Rosowsky, D. Assessing Climate Change Impact on the U.S. East Coast Hurricane Hazard: Temperature, Frequency, and Track. *Nat. Hazards Rev.* **2014**, *15*, 04014001. [CrossRef]
6. Knutson, T.R.; Sirutis, J.J.; Garner, S.T.; Vecchi, G.A.; Held, I.M. Simulated reduction in Atlantic hurricane frequency under twenty-first-century warming conditions. *Nat. Geosci.* **2008**, *1*, 359–364. [CrossRef]
7. Kingston, P.F. Long-term Environmental Impact of Oil Spills. *Spill Sci. Technol. Bull.* **2002**, *7*, 53–61. [CrossRef]
8. Crawley, F.; Tyler, B. *HAZOP: Guide to Best Practice*; Elsevier: Amsterdam, The Netherlands, 2015.
9. Gill, D.A.; Ritchie, L.A.; Picou, J.S. Sociocultural and psychosocial impacts of the exxon valdez oil spill: Twenty-four years of research in Cordova, Alaska. *Extr. Ind. Soc.* **2016**, *3*, 1105–1116. [CrossRef]
10. Palinkas, L.; Downs, M.; Petterson, J.; Russell, J. Social, Cultural, and Psychological Impacts of the Exxon Valdez Oil Spill. *Hum. Organ.* **2008**, *52*, 1–13. [CrossRef]
11. Pine, J. Hurricane Katrina and Oil Spills: Impact on Coastal and Ocean Environments. *Oceanography* **2006**, *19*, 37–39. [CrossRef]
12. Barton, D.C.; Parker, J.V. Finite element analysis of the seismic response of anchored and unanchored liquid storage tanks. *Earthq. Eng. Struct. Dyn.* **1987**, *15*, 299–322. [CrossRef]
13. Haroun, M.A.; Housner, G.W. Earthquake Response of Deformable Liquid Storage Tanks. *J. Appl. Mech.* **1981**, *48*, 411–418. [CrossRef]
14. Niwa, A.; Clough, R.W. Buckling of cylindrical liquid-storage tanks under earthquake loading. *Earthq. Eng. Struct. Dyn.* **1982**, *10*, 107–122. [CrossRef]
15. Sakai, F.; Nishimura, M.; Ogawa, H. Sloshing behavior of floating-roof oil storage tanks. *Comput. Struct.* **1984**, *19*, 183–192. [CrossRef]
16. Merino, R.J.; Brunesi, E.; Nascimbene, R. Probabilistic evaluation of earthquake-induced sloshing wave height in above-ground liquid storage tanks. *Eng. Struct.* **2020**, *202*, 109870. [CrossRef]
17. Ozsarac, V.; Brunesi, E.; Nascimbene, R. Earthquake-induced nonlinear sloshing response of above-ground steel tanks with damped or undamped floating roof. *Soil Dyn. Earthq. Eng.* **2021**, *144*, 106673. [CrossRef]

18. Fabbrocino, G.; Iervolino, I.; Orlando, F.; Salzano, E. Quantitative risk analysis of oil storage facilities in seismic areas. *J. Hazard. Mater.* **2005**, *123*, 61–69. [CrossRef]
19. Salzano, E.; Iervolino, I.; Fabbrocino, G. Seismic risk of atmospheric storage tanks in the framework of quantitative risk analysis. *J. Loss Prev. Process Ind.* **2003**, *16*, 403–409. [CrossRef]
20. Landucci, G.; Antonioni, G.; Tugnoli, A.; Cozzani, V. Release of hazardous substances in flood events: Damage model for atmospheric storage tanks. *Reliab. Eng. Syst. Saf.* **2012**, *106*, 200–216. [CrossRef]
21. Antonioni, G.; Landucci, G.; Necci, A.; Gheorghiu, D.; Cozzani, V. Quantitative assessment of risk due to NaTech scenarios caused by floods. *Reliab. Eng. Syst. Saf.* **2015**, *142*, 334–345. [CrossRef]
22. Khakzad, N.; Van Gelder, P. Fragility assessment of chemical storage tanks subject to floods. *Process Saf. Environ. Prot.* **2017**, *111*, 75–84. [CrossRef]
23. Khakzad, N.; Van Gelder, P. Vulnerability of industrial plants to flood-induced natechs: A Bayesian network approach. *Reliab. Eng. Syst. Saf.* **2018**, *169*, 403–411. [CrossRef]
24. Kameshwar, S.; Padgett, J. Fragility assessment of above ground petroleum storage tanks under storm surge. In Proceedings of the 12th International Conference on Applications of Statistics and Probability in Civil Engineering (ICASP12), Vancouver, BC, Canada, 12–15 July 2015.
25. Kameshwar, S.; Padgett, J.E. Storm surge fragility assessment of above ground storage tanks. *Struct. Saf.* **2018**, *70*, 48–58. [CrossRef]
26. Yang, Y.; Chen, G.; Reniers, G. Vulnerability assessment of atmospheric storage tanks to floods based on logistic regression. *Reliab. Eng. Syst. Saf.* **2020**, *196*, 106721. [CrossRef]
27. Zuluaga Mayorga, S.; Sánchez-Silva, M.; Ramírez Olivar, O.J.; Muñoz Giraldo, F. Development of parametric fragility curves for storage tanks: A Natech approach. *Reliab. Eng. Syst. Saf.* **2019**, *189*, 1–10. [CrossRef]
28. Bernier, C.; Padgett, J.E. Fragility and risk assessment of aboveground storage tanks subjected to concurrent surge, wave, and wind loads. *Reliab. Eng. Syst. Saf.* **2019**, *191*, 106571. [CrossRef]
29. Huang, M.; Chen, G.; Yang, P.; Hu, K.; Zhou, L.; Men, J.; Zhao, J. Multi-hazard coupling vulnerability analysis for buckling failure of vertical storage tank: Floods and hurricanes. *Process Saf. Environ. Prot.* **2022**, *161*, 528–541. [CrossRef]
30. Lan, M.; Shao, Y.; Zhu, J.; Lo, S.; Ng, S.T. A hybrid copula-fragility approach for investigating the impact of hazard dependence on a process facility's failure. *Process Saf. Environ. Prot.* **2021**, *149*, 1017–1030. [CrossRef]
31. Qin, R.; Zhu, J.; Khakzad, N. Multi-hazard failure assessment of atmospheric storage tanks during hurricanes. *J. Loss Prev. Process Ind.* **2020**, *68*, 104325. [CrossRef]
32. Mia, M.M.; Kameshwar, S. Fragility assessment of bottom plates in above ground storage tanks during flood events. *J. Loss Prev. Process Ind.* **2023**, *82*, 104975. [CrossRef]
33. Mia, M.M.; Kameshwar, S. Probabilistic assessment of material failure in anchored above ground storage tanks during flood events. *Eng. Struct.* **2024**, *301*, 117244. [CrossRef]
34. Kameshwar, S.; Padgett, J.E. Fragility and Resilience Indicators for Portfolio of Oil Storage Tanks Subjected to Hurricanes. *J. Infrastruct. Syst.* **2018**, *24*, 04018003. [CrossRef]
35. Bernier, C.; Kameshwar, S.; Elliott, J.R.; Padgett, J.E.; Bedient, P.B. Mitigation strategies to protect petrochemical infrastructure and nearby communities during storm surge. *Nat. Hazards Rev.* **2018**, *19*, 04018019. [CrossRef]
36. 2023 Coastal Master Plan. Available online: https://coastal.la.gov/wp-content/uploads/2023/01/230105_CPRA_MP-Draft_Final-for-web_spreads-main.pdf (accessed on 27 February 2023).
37. NHC Data Archive. Available online: https://www.nhc.noaa.gov/data/ (accessed on 5 July 2023).
38. CERA-Coastal Emergency Risks Assessment. Available online: https://cera.coastalrisk.live/ (accessed on 16 February 2023).
39. Ayyad, M.; Hajj, M.R.; Marsooli, R. Artificial intelligence for hurricane storm surge hazard assessment. *Ocean Eng.* **2022**, *245*, 110435. [CrossRef]
40. Needham, H.F.; Keim, B.D. A storm surge database for the US Gulf Coast. *Int. J. Climatol.* **2012**, *32*, 2108–2123. [CrossRef]
41. Bloemendaal, N.; De Moel, H.; Muis, S.; Haigh, I.D.; Aerts, J.C. Estimation of global tropical cyclone wind speed probabilities using the STORM dataset. *Sci. Data* **2020**, *7*, 377. [CrossRef] [PubMed]
42. *Structural Reliability Analysis and Prediction*, 3rd ed.; Wiley: Hoboken, NJ, USA, 2023; Available online: https://www.wiley.com/en-us/Structural+Reliability+Analysis+and+Prediction,+3rd+Edition-p-9781119265993 (accessed on 22 February 2023).
43. McVay, M.C.; Wasman, S.J.; Consolazio, G.R.; Bullock, P.J.; Cowan, D.G.; Bollmann, H.T. Dynamic soil–structure interaction of bridge substructure subject to vessel impact. *J. Bridge Eng.* **2009**, *14*, 7–16. [CrossRef]
44. Montgomery, D.C. *Design and Analysis of Experiments*, 10th ed.; Wiley: Hoboken, NJ, USA, 2018; Available online: https://www.wiley.com/en-us/Design+and+Analysis+of+Experiments,+10th+Edition-p-9781119492443 (accessed on 4 July 2023).
45. Kontovas, C.A.; Psaraftis, H.N.; Ventikos, N.P. An empirical analysis of IOPCF oil spill cost data. *Mar. Pollut. Bull.* **2010**, *60*, 1455–1466. [CrossRef]
46. The High Price of Heavy Fuel Oil Spills. Ocean Conservancy. Available online: https://oceanconservancy.org/blog/2018/05/03/high-price-heavy-fuel-oil-spills/ (accessed on 30 June 2023).
47. Etkin, D.S. Estimating Cleanup Costs for Oil Spills. *Int. Oil Spill Conf. Proc.* **1999**, *1999*, 35–39. [CrossRef]
48. Etkin, D.S.; Manor, C. Modeling Oil Spill Response and Damage Costs. Available online: https://archive.epa.gov/emergencies/docs/oil/fss/fss04/web/pdf/etkin2_04.pdf (accessed on 13 December 2023).

49. Bureau of Labor Statistics Data. Available online: https://data.bls.gov/timeseries/CUUR0000SA0 (accessed on 15 June 2023).
50. 2014 Assessors Manual Volume II (Commercial and Industrial). Available online: https://www.michigan.gov/treasury/local/stc/assessor-manual/2014-assessors-manual-volume-ii-commercial-and-industrial (accessed on 15 February 2023).
51. API 650: Welded Steel Tanks for Oil Storage. Available online: https://law.resource.org/pub/us/cfr/ibr/002/api.650.2007.pdf (accessed on 27 December 2023).
52. Elfrink, B.; Hanes, D.M.; Ruessink, B.G. Parameterization and simulation of near bed orbital velocities under irregular waves in shallow water. *Coast. Eng.* **2006**, *53*, 915–927. [CrossRef]
53. Bernier, C. Fragility and Risk Assessment of Aboveground Storage Tanks during Storm Events. Ph.D. Thesis, Rice University, Houston, TX, USA, 2019. Available online: https://scholarship.rice.edu/handle/1911/106102 (accessed on 13 February 2023).
54. Introduction-Google Earth User Guide. Available online: http://earth.google.com/intl/ar/userguide/v4/index.htm (accessed on 14 June 2023).
55. Hurricane LAURA Imagery. Available online: https://storms.ngs.noaa.gov/storms/laura/index.html#7/29.862/-93.567 (accessed on 23 February 2023).
56. *ArcGIS Pro 3.2*; Esri Inc.: Redlands, CA, USA; Available online: https://www.esri.com/en-us/arcgis/products/arcgis-pro/overview (accessed on 27 December 2023).
57. 2017 USGS Lidar: Chenier Plain, LA Point Cloud files with Orthometric Vertical Datum North American Vertical Datum of 1988 (NAVD88) Using GEOID18. Available online: https://noaa-nos-coastal-lidar-pds.s3.amazonaws.com/laz/geoid18/8597/index.html (accessed on 23 February 2023).
58. Coastal Engineering Manual. Available online: https://www.publications.usace.army.mil/Portals/76/Publications/EngineerManuals/EM_1110-2-1100_Part-02.pdf (accessed on 13 February 2024).
59. Supplement 2 for Minimum Design Loads and Associated Criteria for Buildings and Other Structures (ASCE/SEI 7-22). Available online: https://ascelibrary.org/doi/epdf/10.1061/9780784415788.sup2 (accessed on 14 February 2024).
60. Bursi, O.S.; Abbiati, G.; Caracoglia, L.; Salandra, V.L.; Filippo, R.D.; Reza, M.S. Dynamic Response of Coupled Tanks and Piping Systems Under Seismic Loading. In Proceedings of the ASME 2015 Pressure Vessels and Piping Conference, Boston, MA, USA, 19–23 July 2015. [CrossRef]
61. Vathi, M.; Karamanos, S.A.; Kapogiannis, I.A.; Spiliopoulos, K.V. Performance Criteria for Liquid Storage Tanks and Piping Systems Subjected to Seismic Loading. *J. Press. Vessel Technol.* **2017**, *139*, 051801. [CrossRef]
62. Tarasenko, A.; Chepur, P.; Gruchenkova, A. Stress-strain state of the pipe-tank system under tank bottom settlement. *J. Phys. Conf. Ser.* **2019**, *1145*, 012005. [CrossRef]
63. Bursi, O.S.; Abbiati, G.; Caracoglia, L.; Reza, M.S. Effects of Uncertainties in Boundary Conditions on Dynamic Characteristics of Industrial Plant Components. In Proceedings of the ASME 2014 Pressure Vessels and Piping Conference, Anaheim, CA, USA, 20–24 July 2014. [CrossRef]
64. Beyer, J.; Trannum, H.C.; Bakke, T.; Hodson, P.V.; Collier, T.K. Environmental effects of the Deepwater Horizon oil spill: A review. *Mar. Pollut. Bull.* **2016**, *110*, 28–51. [CrossRef] [PubMed]

Disclaimer/Publisher's Note: The statements, opinions and data contained in all publications are solely those of the individual author(s) and contributor(s) and not of MDPI and/or the editor(s). MDPI and/or the editor(s) disclaim responsibility for any injury to people or property resulting from any ideas, methods, instructions or products referred to in the content.